

DNA-directed synthesis of zinc oxide nanowires on carbon nanotube tips

Adam D Lazareck¹, Sylvain G Cloutier¹, Teng-Fang Kuo¹,
Bradford J Taft², Shana O Kelley² and Jimmy M Xu¹

¹ Division of Engineering, Brown University, Providence, RI 02912, USA

² Department of Chemistry, Boston College, Chestnut Hill, MA 02467, USA

E-mail: Adam.Lazareck@brown.edu

Received 17 January 2006

Published 5 May 2006

Online at stacks.iop.org/Nano/17/2661

Abstract

This paper describes a class of three component hybrid nanowires templated by DNA directed self-assembly. Through the modification of carbon nanotube (CNT) termini with synthetic DNA oligonucleotides, gold nanoparticles are delivered, via DNA hybridization, to CNT tips that then serve as growth sites for zinc oxide (ZnO) nanowires. The structures we have generated using DNA templating represent an advance toward building higher order sequenced one dimensional nanostructures with rational control.

(Some figures in this article are in colour only in the electronic version)

The rational self-assembly of nanostructured materials is a powerful means of bottom-up nanofabrication [1, 2]. Incorporating the specificity of biological molecules for nanostructure production offers the possibility of encoding instructional information for the assembly, but its application has been limited to simple structures whose constituent materials are of uniform composition [3, 4]. We report here a new class of three-component hybrid nanowires templated by biological self-assembly. Nanowires with heterogeneous composition are of great interest due to their potential use as electronic or optoelectronic components, but it is difficult to fabricate such structures by conventional top-down techniques [5, 6]. A system is described here that relies on the site-specific attachment of a DNA oligonucleotide to arrayed nanostructures. The subsequent delivery of a catalyst through hybridization of a complementary sequence provides a platform for the growth of a second type of nanowire, and is an inherently parallel and scalable process thus addressing a main challenge of multi-material nanowire fabrication [7]. The approach described here is the first to generate a one dimensional, optically active, multi-material nanowire platform using site specific catalyst placement via biological self-assembly [8].

The strategy we have developed for the generation of hybrid nanostructures uses arrayed carbon nanotubes (CNTs) as a platform. CNTs represent an ideal scaffold for precise integration of both synthetic and biological nanostructures as they can be generated in arrays with variable spacing and

height, and the structures are mechanically strong. Moreover, CNTs can be modified with site specificity, as their closed sidewalls and open ends exhibit inherently different physical and chemical properties [9, 10]. Nitric acid etching introduces carboxylic groups at defect sites (primarily at the tips), while the hydrophobic graphitic sidewalls are chemically inert. Therefore, the tips can be modified to allow for the construction of hybrid materials [11]. In this work, carbon nanotube (CNT) termini are modified site-specifically with gold nanoparticles via DNA hybridization, with the nanoparticles serving as subsequent growth sites for zinc oxide (ZnO) nanowires. ZnO is both a robust demonstration vehicle and a multifunctional optoelectronic [12, 13]/piezoelectric material [14, 15]. Previous attempts to perform ZnO nanowire growth on CNTs, in the absence of encoded site selection, have resulted in randomly oriented ZnO wires [16]. The structures we have generated using DNA templating represent an advance toward building higher order sequenced one dimensional nanostructures with rational control.

Highly ordered CNT arrays are generated through the growth of multiwalled nanotubes (MWNTs) within an aluminium oxide nanopore template [17, 18]. Nanotubes were exposed by wet etching the aluminium oxide template in a 6% H₃PO₄, 1.8% CrO₃ solution for 5 h at 25 °C, yielding 40 nm of exposed CNTs. The template defines the geometric features of the CNT array, and in the studies described here the CNTs are 50 nm in diameter and have walls of 3 nm thickness, a total length of 10 μm, and a centre-to-centre

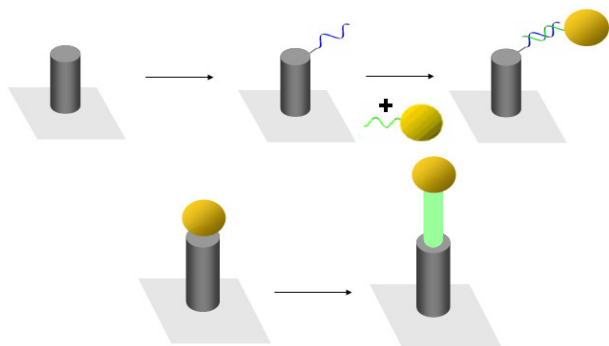


Figure 1. Scheme 1: ZnO–CNT hybrid nanostructures from DNA sequence dependent catalyst placement. Sequence A is attached to carboxylic acid functional groups displayed at the ends of CNTs through amide coupling. Sequence B, carrying a 20 nm Au particle as a label, is hybridized to sequence A previously bound to the CNTs. ZnO nanowires are grown from the Au catalyst using standard conditions, resulting in hybrid nanostructures where the catalyst was placed by sequence specific hybridization.

spacing of 100 nm between adjacent tubes. DNA synthesis was performed using standard solid-phase techniques [19]. Amine- and thiol-modified oligonucleotides were prepared and purified by reverse phase HPLC as previously reported [11].

DNA sequences were as follows:

sequence A: NH₂-5GATAGTCATCATCAA

sequence B: SH-5TTGATGATGACTATC.

Nanoparticle-labelled single-stranded DNA was prepared following established protocols [20]. Nanoparticles (Ted Pella), were stabilized using bis(p-sulfonatophenyl)phenylphosphine dihydrate dipotassium salt (Strem Chemicals). After stabilization, nanoparticles were precipitated from solution by adding solid sodium chloride until a blue colour change was observed. The nanoparticles were then pelleted and resuspended in a smaller volume to produce a concentration of 450 nM. Gold nanoparticle–DNA conjugates (sequence B) were formed by incubating molar equivalents of DNA and nanoparticles in 25 mM sodium chloride. Typical incubation periods ranged from 8 to 16 h. Prior to the deposition of single-stranded amine-terminated DNA (sequence A), carboxyl groups on the CNT array were exposed by acid-washing for 1 h in 50% H₂SO₄:HNO₃ (3:1) in H₂O. Amide coupling proceeded as follows: 10 eq. of TSTU (Advanced Chemtech), approximately 1 mg per CNT surface, and 5 eq. DIEA (1 ml) in 10 ml DMF was introduced to the CNT sample and incubated for 15 min. Next, 10 mM amino-modified DNA in 50 mM sodium phosphate buffer (pH 8) was introduced in 10 ml for each sample and left to incubate for an additional 15 min in the presence of the original DMF solvent. The sample was then washed in water and placed in buffer solution for hybridization.

Hybridization of the gold-nanoparticle DNA conjugates to probe strands immobilized on the CNT array occurred in 25 mM NaCl, 50 mM phosphate buffer at pH 7. The arrays were immersed in a solution of 100 nM Au–DNA conjugates in the same buffer, heated to 45 °C, and allowed to slowly cool to room temperature. Once cooled to room temperature, the samples were stringently washed in the same buffer, and dried in argon gas.

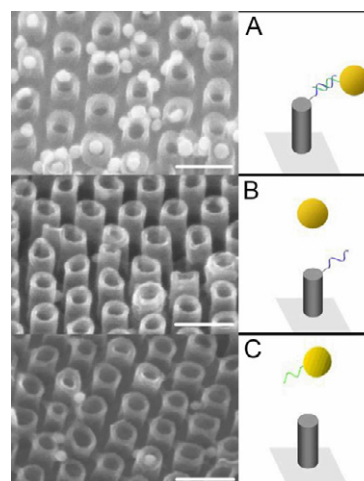


Figure 2. Scanning electron micrograph of a CNT array following step 2 of scheme 1. (A) A high specificity is observed for the tips of the nanotubes, with some tubes displaying successful hybridization of up to three labelled sequences. (B) is a control image of unmodified nanoparticles deposited on CNTs modified with sequence A, and (C) exhibits minimal non-specific adsorption in the absence of the DNA anchor strand, sequence A. The scale bar represents 100 nm.

ZnO nanowires were grown on the nanoparticle–DNA–CNT samples in a tube furnace at 600 °C using a ZnAs₂ source as the zinc supply. A 3 inch long ceramic boat carrying both the sample and the ZnAs₂ source was transferred into a 1 inch diameter horizontal tube. Argon gas flowing at 100 sccm carried the Zn vapour, and the chamber was left at atmospheric pressure to use the air as an oxygen source. A growth time of 7 min resulted in ZnO nanowires with an average length of 200 nm.

Photoluminescence spectra were generated using a Spectra-Physics continuous wave argon-ion laser at an excitation wavelength of 351 nm. The emission was collected with a Jobin Yvon Fluorolog spectrometer. All scanning electron microscope images were taken with an LEO-1530 SEM. Electron dispersive spectra were collected from an Oxford Instruments INCAx-sight EDS. The overall strategy is depicted in figure 1.

Figure 2(A) shows the CNTs after DNA attachment via amide coupling and following the hybridization of the complementary 15-mer attached to a gold nanoparticle label. Importantly, the nanoparticles are localized at the tips of the CNTs, where the majority of the carboxylic acids are expected to be found [21]. Figure 2(B) displays a control experiment without sequence B on the nanoparticle, and figure 2(C) shows the sequence B modified nanoparticle control, in the absence of sequence A. While each control experiment exhibited a minimal amount of non-specific interaction, possible sources of non-specific linking could be due to electrostatic interactions between the CNT's carboxyl groups and the charged ligand species used to stabilize gold colloids [22] (in the case of 2(B)) or the charged DNA backbone (in the case of 2(C)). In either case, thorough buffer washing is capable of removing the majority of nanoparticles non-specifically directed to the CNT sample.

By taking advantage of the unique platform produced by specific placement of a catalyst at the nanotube tips,



Figure 3. Scanning electron micrograph of three different CNT–ZnO hybrid structures at varying tilt angles. (A) SEM tilt angle 45°. (B) An overhead view. (C) A 30° tilt angle. The scale bar represents 50 nm.

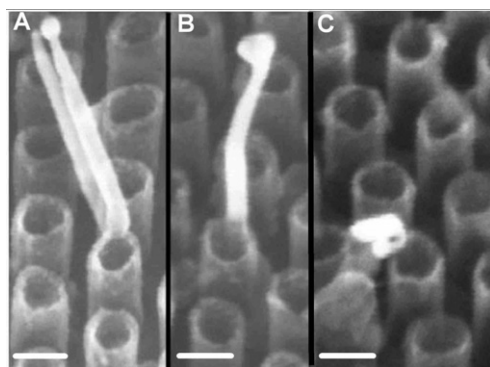


Figure 4. (A) and (B) Scanning electron micrographs of CNT–ZnO hybrid structures with an SEM tilt angle of 30°. While not all nanotubes display ZnO nanowires, no nanowires are observed which are not attached to CNTs. (C) Scanning electron micrograph after ZnO growth step from figure 2(C)'s non-specific adsorption control experiment. Scale bars represent 100 nm.

ZnO nanowires were grown sequentially from arrayed CNTs [16, 23]. After delivery of gold nanoparticle catalyst to the CNT tips, all DNA was vaporized at the 600 °C ZnO growth step.

Figures 3, 4(A) and (B) illustrate some representative nanotubes after ZnO growth, and photoluminescence (PL) spectra from these samples exhibited peaks typical of ZnO nanowires as shown in figure 6 (top curve) [24]. The high ultraviolet-to-green emission ratio observed from nanowires grown on CNTs implies a high crystalline quality, as the green-band emission is an indicator of crystalline defects, in this case oxygen vacancies, in the ZnO nanowires [24, 25]. The chemical constituents of the resulting ZnO–CNT structures were verified by EDS as represented in figure 5.

We attempted to grow ZnO nanowires from figure 2(C)'s control samples, but did not observe a ZnO photoluminescence signature (figure 6, bottom curve) or any ZnO nanowires from these samples under SEM, as in figure 4(C).

Typical catalytic growth techniques require temperatures in excess of 900 °C to grow ZnO nanorods [26, 27]. At

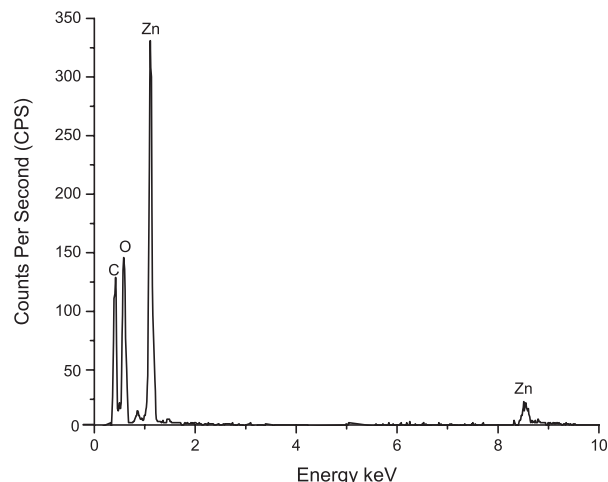


Figure 5. EDS spectra of ZnO–CNT sample. EDS spectra of other ZnO–CNT samples are the same except slight differences in the relative intensities.

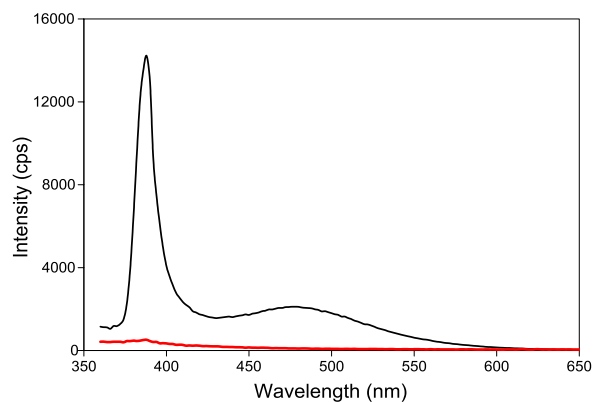


Figure 6. Photoluminescence spectra of ZnO–CNT sample (top curve) and control sample (bottom curve).

these temperatures, diffusion and migration of gold catalyst nanoparticles on flat surfaces could mitigate the effect of site specific placement. However, in this case, with the CNT tip's surface topology and lower relative growth temperature of 600 °C, no discernable mobility of the nanoparticles from the CNT termini was observed.

One of the main differences in the distribution of nanoparticles before the ZnO growth step, and the distribution of nanowires after synthesis, is in the average number of gold nanoparticles per CNT before growth, and the average number of ZnO nanowires per CNT after the growth step. After qualitatively assessing the SEM images, we observed, on average, between 1 and 4 nanoparticles per functionalized CNT tip before growth compared to one and rarely two ZnO nanowires per CNT after growth. Therefore, the apparent yield for ZnO nanowire growth would be 25–50%.

A significant implication of this system is the sequential integration of three dimensional heteromaterial nanostructures. These hybrid material nanostructures can also act as a platform for electro-optical/piezoelectric devices. All of these possibilities are enabled by DNA's unrivalled specificity to deliver a site-specific catalyst payload to the CNT tips,

and thereby serves as a biologically assisted nanostructure fabrication paradigm.

Acknowledgments

This work is supported by AFOSR, MURI and DARPA. ADL and SGC are also grateful to NSERC for its fellowship support.

References

- [1] Li M, Mann S and Schnablegger H 1999 *Nature* **402** 393–5
- [2] Lopes W A and Jaeger H M 2001 *Nature* **414** 735–8
- [3] Braun E, Eichen Y, Sivan U and Ben-Yoseph G 1998 *Nature* **391** 775–8
- [4] Li Y, Tseng Y, Kwon S, Espaux L D, Bunch J S, Mceuen P L and Luo D 2004 *Nat. Mater.* **3** 38–42
- [5] Hu J, Odom T W and Lieber C M 1999 *Acc. Chem. Res.* **32** 435
- [6] Dekker C 1999 *Phys. Today* **52** 22
- [7] Lauthon L J, Gudixsen M S and Lieber C M 2004 *Phil. Trans. R. Soc. A* **362** 1247–60
- [8] Hu J, Ouyang M, Yang P and Lieber C M 1999 *Nature* **399** 48–51
- [9] Saito R, Dresselhaus G and Dresselhaus M S 1998 *Physics of Carbon Nanotubes* (London: Imperial College Press)
- [10] Dresselhaus M S, Dresselhaus G and Avouris P 2001 *Carbon Nanotubes: Synthesis, Structure, Properties and Applications* (Berlin: Springer)
- [11] Taft B J, Lazareck A D, Withey G D, Yin A, Xu J M and Kelley S O 2004 *J. Am. Chem. Soc.* **126** 12750–1
- [12] Jeong M C, Oh B Y, Lee W and Myoung J M 2005 *Appl. Phys. Lett.* **86** 103105/1–3
- [13] Lin C C, Chen H P and Chen S Y 2005 *Chem. Phys. Lett.* **404** 30–4
- [14] Kong X Y and Wang Z L 2003 *Nano Lett.* **3** 1625
- [15] Kong X Y, Ding Y, Yang R S and Wang Z L 2004 *Science* **303** 1348
- [16] Kim H and Sigmund W 2002 *Appl. Phys. Lett.* **81** 2085–7
- [17] Li J, Papadopoulos C, Xu J M and Moskovits M 1999 *Appl. Phys. Lett.* **75** 367–9
- [18] Papadopoulos C, Chang B H, Yin A J and Xu J M 2002 *Int. J. Nanosci.* **1** 205–12
- [19] Taft B J, Lapierre-Devlin M A and Kelley S O 2006 *Chem. Commun.* **9** 962–4
- [20] Loweth C J, Caldwell W B, Peng X, Alivisatos A P and Schultz P G 1999 *Angew. Chem. Int. Edn* **38** 1808–12
- [21] Tsang S C, Chen Y K, Harris P J F and Green M L H 1994 *Nature* **372** 159–62
- [22] Kim T, Lee K, Gong M S and Joo S W 2005 *Langmuir* **21** 9524–8
- [23] Cassell A M, Li J, Stevens R M D, Koehne J E, Delzeit L, Ng H T, Ye Q, Han J and Meyyappan M 2004 *Appl. Phys. Lett.* **85** 2364–6
- [24] Chik H, Liang J, Cloutier S G, Kouklin N and Xu J M 2004 *Appl. Phys. Lett.* **84** 3376–8
- [25] Huang M H, Wu Y, Feick H, Tran N, Weber E and Yang P 2001 *Adv. Mater.* **13** 113–6
- [26] Huang M H, Wu Y, Feick H, Tran N, Weber E and Yang P 2001 *Adv. Mater.* **13** 113–6
- [27] Wan Q, Li Q H, Chen Y J, Wang T H, He X L, Gao X G and Li J P 2004 *Appl. Phys. Lett.* **84** 3085–7